ELSEVIER

Journal of Fluids and Structures 25 (2009) 567–585

JOURNAL OF FLUIDS AND STRUCTURES

www.elsevier.com/locate/jfs

A coupled BE–FE study for evaluation of seismically isolated cylindrical liquid storage tanks considering fluid–structure interaction

M.R. Shekari, N. Khaji*, M.T. Ahmadi

Civil Engineering Department, Tarbiat Modares University, P.O. Box 14115-143, Tehran, Iran

Received 2 January 2008; accepted 11 July 2008
Available online 20 December 2008

Abstract

The effects of base-isolation on the seismic response of cylindrical vertical flexible liquid storage tanks subjected to horizontal seismic ground motion are presented in this paper. The whole system consists of two main parts: the base-isolation component, and the fluid–structure interaction subsystem. Dynamic analysis of liquid storage tank is achieved through the use of finite shell elements for the structure and internal boundary elements for the liquid region. The boundary element equations are employed to obtain an equivalent liquid mass matrix which is then coupled with the shell structure mass matrix, resulting in the coupled equations of motion. Finally, the coupled equations of motion are connected with the base-isolation system to observe the whole system behavior. A bilinear hysteretic element is used to illustrate the base-isolation system. The analysis is performed in the time domain in which, hydrodynamic interaction is taken into account. It is shown that the seismic response of the isolated tank could be significantly reduced compared with the fixed-foundation tanks. Parametric studies are carried out to study the effects of different system parameters on the effectiveness of the base-isolation system. These parameters are the tank geometry aspect ratio (height to radius), the flexibility of the isolation system, the liquid surface displacement variations, and the tank wall flexibility. It is observed that the seismic isolation is more effective in slender tanks in comparison with broad tanks. Furthermore, it is shown that the isolation efficiency is partially more significant in rigid tanks. It is also noticeable that flexible isolators considerably reduce the seismic response in comparison with stiff isolators. Despite the foregoing advantages, liquid surface displacement increases due to seismic isolation, especially in slender tanks.

Keywords: Seismic response; Base-isolation; Liquid storage tanks; Fluid–structure interaction; Boundary elements; Finite elements

1. Introduction

The dynamic behavior of a liquid storage tank as a special structure differs from those of general structures. The cylindrical shape of these important structures is used to store vital products, such as petroleum products for cities and industrial facilities. Damage to these structures during a strong ground motion may lead to fire or other hazardous events. In the last decade, many strong earthquakes such as the 1990 Luzon earthquake (Philippines), the 1994

*Corresponding author. Tel.: +98 21 82883319; fax: +98 21 82883381.
E-mail address: nkhaji@modares.ac.ir (N. Khaji).

0889-9746/$ - see front matter © 2008 Elsevier Ltd. All rights reserved.
doi:10.1016/j.jfluidstructs.2008.07.005

Northridge earthquake (USA), and the 1995 Kobe earthquake (Japan), have occurred and caused severe damage to the liquid storage tanks. The most common damages such as Diamond-shaped buckling (Shrimali and Jangid, 2002), Elephants-foot buckling, tank's roof buckling and tank uplifting (Malhotra and Veletsos, 1994) mainly caused by the hydrodynamic pressure acting on the tank wall. Therefore, seismic analysis of such tanks should be taken into account to calculate the hydrodynamic pressure more precisely, and appropriate methods are proposed to reduce these damages.

In the first proposed analysis procedure of tanks containing liquid, the tank wall and foundation were assumed to be rigid (Housner, 1963). By this assumption, the hydrodynamic pressure acting on the tank wall is split into two components: the impulsive pressure resulting from the liquid mass accelerating due to the ground acceleration, and the convective pressure due to sloshing (liquid surface displacement). In 1964, the Alaska earthquake caused damage to a large number of ground-supported cylindrical tanks. This earthquake revealed the importance of tank wall flexibility in amplifying the impulsive component of the hydrodynamic pressure. Employing numerical analysis results for the liquid-tank problem, Haroun and Ellaithy (1985) developed the previous model of Housner (1963) by adding the effect of tank wall flexibility. More analyses of the dynamic behavior of liquid-filled cylindrical tanks were carried out by Veletsos and Tang (1987) and Malhotra et al. (2000), considering horizontal base excitation. Some researchers investigate the response of partially filled liquid tanks to consider fluid–structure interaction, analytically [e.g., Amabili et al. (1998), Papaspyrou et al. (2004)]. Seismic design procedures for elevated tanks were examined by Livaoğlu and Doganğün (2006) considering both mechanical and finite-element modeling techniques. Liquid non-uniformity effects on the response of liquid tanks were investigated by Tang (1994) and Shivakumar and Veletsos (1995). Also seismic response of tanks containing layered liquids was studied specifically with respect to sloshing, chiefly in rigid tanks (Veletsos and Shivakumar, 1993, 1995). The sloshing effect is commonly taken into account by employing the linear Bernoulli equation. As a new result, the large amplitude sloshing in a liquid tank was investigated considering rigid walls (Haroun and Chen, 1996). Several analytical and numerical solutions have been developed considering the interaction between fluid and flexible tank walls (Haroun and Housner, 1981, 1982).

To protect the liquid storage tanks against the possible hazard of earthquakes, they may regularly be strengthened which results in higher magnitude of seismic energy attraction. The other technique for this purpose is base-isolation. Seismic isolation is achieved by installing certain isolation devices to decouple the structure from the ground to reduce peak responses of the structure. In this case, the superstructure may usually be expected to exhibit linear elastic behavior under the excitation of severe earthquakes. In a first attempt to study this subject, Chalhoub and Kelly (1990) noticed that the sloshing response increases, while the total hydrodynamic pressure and base reaction considerably decreases due to the base-isolation of the liquid tanks. Also, Liang and Tang (1994) observed the effect of base-isolation on the hydrodynamic pressure variations. Kim and Lee (1995) employed a pseudodynamic test to evaluate the seismic performance of base-isolated liquid storage tanks. Using a lumped-mass-stick model to represent the tank-liquid system, Malhotra (1997a) observed the effects of base-isolation on seismic response of vertical cylindrical liquid storage tanks. Malhotra (1997b) investigated the effects of base-isolation on both impulsive and convective components of pressure, for two steel tanks (one broad and one slender). An analytical solution supposing the whole system as a three-degree-of-freedom model was developed by Shenton and Hampton (1999) to investigate the seismic response of isolated elevated water tanks. Jadhav and Jangid (2004) studied the seismic response of liquid storage tanks isolated by elastomeric bearings and sliding system under real earthquakes. The continuous liquid mass of the tank was modeled as sloshing, impulsive and rigid lumped masses. This model was recently employed to examine the response of base-isolated liquid storage tanks to near-fault motions (Jadhav and Jangid, 2006). Various important parameters (e.g., aspect ratio of tank, the period of isolation and the damping of isolation bearings) were considered in this study. Numerical methods have been recently employed to study the effects of base-isolation systems on the response of liquid storage tanks [see, e.g., Kim et al. (2002), Cho et al. (2004)]. Recently, Shrimali and Jangid (2002, 2004) studied the seismic response of liquid storage tanks under seismic excitation, considering the effects of some parameters of base-isolation system.

The main purpose of this study is to organize an efficient numerical procedure to analyze the effect of base-isolation on the seismic response of liquid storage tanks, considering the influence of various tank and isolation system parameters. To take into account the fluid–structure interaction phenomenon, the liquid region is modeled by internal boundary elements, which reduce the three-dimensional fluid problem into a two-dimensional-surface one. This reduction may be performed by transforming the governing partial differential equation of the three-dimensional fluid body into an integral equation that corresponds only to boundary values (Brebbia and Dominguez, 1992). The structure is modeled by three-dimensional finite shell elements, which easily model the arbitrary shape of the tank wall. Biaxial hysteric members are used to simulate the base-isolation system (Kelly, 1993). Thanks to intrinsic non-linear behavior of the whole system (i.e., hydrodynamic interaction problem coupled with base-isolation) dynamic response, the most straightforward approach may be considered as the time domain analysis of BE–FE formulation (Cho et al., 2004). Since the time domain formulation of BEM is more complicated in comparison with the frequency domain

formulation (Brebbia and Dominguez, 1992), the latter has been selected to construct the coupled formulation in this research. The frequency domain formulations of BE–FE methods make more accurate sense for the hydrodynamic pressure component due to the sloshing effect, which depends very strongly on the frequency spectrum of the ground motion. This frequency domain analysis (i.e., forward and inverse Fourier transformations) is performed for very short consecutive time steps of ground motion time history to permit the algorithm to follow the correct path of a non-linear phenomenon. Thereafter, the effects of the base-isolation system on the seismic response of liquid storage tanks are comprehensively analyzed.

2. Formulation of seismically isolated liquid tank on rigid foundation

A numerical procedure based on a hybrid formulation, which combines the finite shell elements for the structure and the internal boundary elements for the liquid region is developed in time domain. As shown in Fig. 1, the whole system is made up of two main parts: the fluid–structure interaction subsystem and the seismic isolation component. The seismic isolation subsystem is modeled by rubber bearing which is a steel-reinforced material whose behavior is shown in Fig. 2 (Kelly, 1993).

2.1. BEM formulation for the fluid domain

In this investigation, it is assumed that the fluid is ideal, i.e., inviscid and incompressible, and its motion is irrotational. Hence, the governing equation of liquid motion is represented by the Laplace equation,

$$\nabla^2\phi(x,y,z,t)=0, \tag{1}$$

where ϕ is the velocity potential. The boundary element method is used to solve the Laplace equation with the following boundary conditions (Fischer and Rammerstorfer, 1999):

(a) Dynamic and kinematic boundary condition of the free surface:

$$\frac{\partial^2\phi}{\partial t^2}+g\frac{\partial\phi}{\partial z}=0; \tag{2}$$

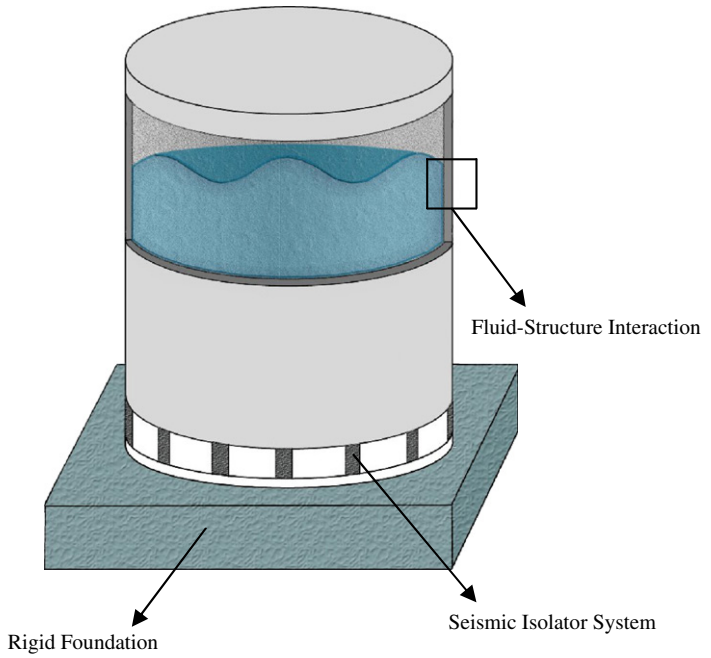

Fig. 1. Seismically isolated cylindrical liquid storage tank on rigid foundation.

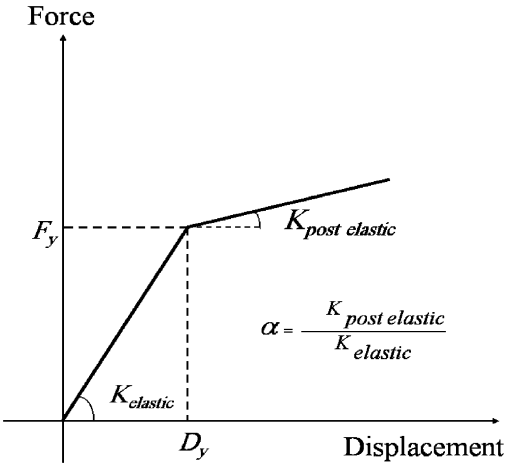

Fig. 2. Base isolator horizontal stiffness modeling.

(b) Boundary condition of the fluid–structure interface:

$$\frac{\partial \phi}{\partial n} = v_n(t), \tag{3}$$

in which g is the gravitational acceleration, and $v_n(t)$ the relative normal fluid velocity at the tank wall at time t.

The linearized Bernoulli equation for pressure represents the hydrodynamic pressure acting on the tank wall

$$P = -\rho \frac{\partial \phi}{\partial t}. \tag{4}$$

Furthermore, the hydrodynamic pressure at the free surface is

$$P = \rho g \eta(x, y, t), \tag{5}$$

where $\eta(x,y,t)$ is the sloshing height, and ρ the mass density of the liquid.

The boundary element method is used to solve the motion of liquid in discretized form, as follows (Brebbia and Dominguez, 1992):

$$\mathbf{H}\boldsymbol{\phi} = \mathbf{G}\mathbf{q}, \tag{6}$$

in which $\mathbf{H}$ and $\mathbf{G}$ indicate boundary element coefficient matrices for the potential vector $\boldsymbol{\phi}$, and the flux vector $\mathbf{q}$, respectively. Assuming harmonic motion in the frequency domain, the boundary element Eq. (6) for the fluid region may be rewritten and separated into the following expressions, according to the fluid surface and tank nodes (Lay, 1993):

$$\mathbf{p}_t = \rho \omega^2 \mathbf{B}_{\mathrm{I}}^{-1} \mathbf{B}_{\mathrm{II}} \mathbf{u}_t, \tag{7}$$

$$\mathbf{p}_f = \rho g \mathbf{u}_f, \tag{8}$$

in which the subscripts t and f denote the nodes on the tank wall and liquid free surface, respectively, and ω is an independent variable in the transformed frequency domain. The matrices $\mathbf{B}_{\mathrm{I}}$ and $\mathbf{B}_{\mathrm{II}}$ can be formulated as

$$\mathbf{B}_{\mathrm{I}} = \mathbf{H}_{tt} + \omega^2 \mathbf{G}_{tf} \mathbf{D}^{-1} \mathbf{H}_{ft} - g \mathbf{H}_{tf} \mathbf{D}^{-1} \mathbf{H}_{ft}, \quad \mathbf{B}_{\mathrm{II}} = \mathbf{G}_{tt} + \omega^2 \mathbf{G}_{tf} \mathbf{D}^{-1} \mathbf{G}_{ft} - g \mathbf{H}_{tf} \mathbf{D}^{-1} \mathbf{G}_{ft}, \tag{9,10}$$

whereas, if sloshing is ignored, they become

$$\mathbf{B}_{\mathrm{I}} = \mathbf{H}_{tt} - \mathbf{G}_{tf} \mathbf{G}_{ff}^{-1} \mathbf{H}_{ft}, \quad \mathbf{B}_{\mathrm{II}} = \mathbf{G}_{tt} - \mathbf{G}_{tf} \mathbf{G}_{ff}^{-1} \mathbf{G}_{ft}, \tag{11,12}$$

where

$$\mathbf{D}^{-1} = g \mathbf{H}_{ff} - \omega^2 \mathbf{G}_{ff}^{-1}. \tag{13}$$

The hydrodynamic pressure vector $\mathbf{p}_t$ is considered as the external pressure vector that is converted into the equivalent nodal forces exerted on the shell structure. The conversion is done by introducing the shape function

matrix $\mathbf{N}$. Then the nodal force vector $\mathbf{f}_t$ may be written in terms of hydrodynamic pressure vector $\mathbf{p}_t$ as

$$\mathbf{f}_t = \mathbf{N}\mathbf{p}_t. \tag{14}$$

Substituting Eq. (7) into Eq. (14), the following expression is obtained:

$$\mathbf{f}_t = \omega^2 \mathbf{M}^L \mathbf{u}_t, \tag{15}$$

where $\mathbf{M}^L$ is equivalent liquid mass matrix given by

$$\mathbf{M}^L = \rho \mathbf{N} \mathbf{B}_{\mathrm{I}}^{-1} \mathbf{B}_{\mathrm{II}}. \tag{16}$$

Note that if free-surface sloshing is considered, $\mathbf{M}^L$ is frequency dependent also. Then the problem should be solved in the frequency domain. In other words, modeling the hydrodynamic pressure component due to sloshing effect depends too much on the frequency spectrum of the ground motion. Therefore, it seems useful to model the liquid free surface in the frequency domain.

2.2. FEM formulation for the structure domain

Considering the ground acceleration as an external excitation, the equation of motion for the shell structure can be written in matrix form as follows [see, e.g., Zienkiewicz and Taylor (2000)]:

$$\mathbf{M}^S \ddot{\mathbf{u}}(t) + \mathbf{C}^S \dot{\mathbf{u}}(t) + \mathbf{K}^S \mathbf{u}(t) = \mathbf{F}(t), \tag{17}$$

where $\mathbf{M}^S$, $\mathbf{K}^S$ and $\mathbf{C}^S$ are the mass, stiffness, and damping matrices of the shell structure, respectively. Also, $\ddot{\mathbf{u}}(t)$, $\dot{\mathbf{u}}(t)$, and $\mathbf{u}(t)$ are the nodal accelerations, velocities, and displacements of the structure, respectively. $\mathbf{F}(t)$ denotes the force vector for ground excitation and for the fluid–structure interaction system. To analyze the equation of motion in the frequency domain, Eq. (17) is represented by the following equation:

$$(\mathbf{K}^S + \mathrm{i}\omega \mathbf{C}^S - \omega^2 \mathbf{M}^S)\mathbf{u}(\omega) = \mathbf{F}(\omega), \tag{18}$$

in which $\mathbf{u}(\omega)$ and $\mathbf{F}(\omega)$ are the magnitude of nodal displacements and forces in the frequency domain.

2.3. Fluid–structure equation of motion with fixed base

In order to perform the dynamic analysis of liquid storage tanks, the equation of motion of the whole system should be solved. To carry out the analysis in the frequency domain, the nodal displacement vector $\mathbf{u}(\omega)$ is separated into the displacement vector of fluid–structure interface nodes $\mathbf{u}_t$ and the liquid-free-surface node vector $\mathbf{u}_f$ only. The governing set of equations of the fluid–structure system is obtained by coupling the equations of each region using the equilibrium conditions and compatibility conditions at the interfaces as follows (Kelly, 1993):

$$(\mathbf{K} + \mathrm{i}\omega \mathbf{C} - \omega^2 \mathbf{M})\mathbf{u}(\omega) = -\mathbf{M}\mathbf{r}\hat{\ddot{\mathbf{u}}}_g(\omega), \tag{19}$$

where

$$\mathbf{K} = \begin{bmatrix} \mathbf{K}_{tt}^S + \mathbf{K}_{tt}^L & \mathbf{K}_{tf}^L \\ \mathbf{0} & \mathbf{K}_{ff}^L \end{bmatrix}, \quad \mathbf{C} = \begin{bmatrix} \mathbf{C}_{tt}^S + \mathbf{C}_{tt}^L & \mathbf{C}_{tf}^L \\ \mathbf{0} & \mathbf{C}_{ff}^L \end{bmatrix}, \quad \mathbf{M} = \begin{bmatrix} \mathbf{M}_{tt}^S + \mathbf{M}_{tt}^L & \mathbf{M}_{tf}^L \\ \mathbf{M}_{ft}^L & \mathbf{M}_{ff}^L \end{bmatrix}, \tag{20a,b,c}$$

$$\mathbf{u} = [\,\mathbf{u}_t \quad \mathbf{u}_f\,]^{\mathrm{T}}, \tag{20d}$$

and $\hat{\ddot{\mathbf{u}}}_g(\omega)$ denotes the ground acceleration amplitude vector in the frequency domain, which is obtained by applying the Fourier transformation technique on an earthquake time history. Also, $\mathbf{r}$ is the transformation vector that couples each degree of freedom to the ground motion.

The unknown vector $\mathbf{u}(\omega)$ is calculated for a range of frequencies, and then using the inverse Fourier transformation it may be converted into the time domain to obtain the time-history vector $\mathbf{u}(t)$.

2.4. Base-isolated liquid storage tank on a rigid foundation

To obtain the dynamic response of this system, the liquid storage tank should be connected with the foundation using the base-isolation system. This task may easily be carried out by modification of Eq. (19), in which new characteristics matrices are introduced. Here, base-isolation dynamic effects are taken into account in the overall system behavior. As

a result, the governing equations of motion for superstructure and the base-isolation may be written as

$$(\mathbf{K}^* + i\omega\mathbf{C}^* - \omega^2\mathbf{M}^*)\mathbf{u}^*(\omega) = -\mathbf{M}^*\mathbf{r}\hat{\ddot{u}}_g(\omega), \tag{21}$$

in which new characteristic matrices are

$$\mathbf{K}^* = \begin{bmatrix} \mathbf{k}_b & \mathbf{0} \\ \mathbf{0} & \mathbf{K} \end{bmatrix}, \quad \mathbf{C}^* = \begin{bmatrix} \mathbf{c}_b & \mathbf{0} \\ \mathbf{0} & \mathbf{C} \end{bmatrix}, \quad \mathbf{M}^* = \begin{bmatrix} \mathbf{r}^T\mathbf{M}\mathbf{r} + \mathbf{m}_b & \mathbf{r}^T\mathbf{M} \\ \mathbf{M}\mathbf{r} & \mathbf{M} \end{bmatrix}, \tag{22a,b,c}$$

$$\mathbf{u}^* = [\,\mathbf{u}_b \quad \mathbf{u}_t \quad \mathbf{u}_f\,]^T, \tag{22d}$$

where $\mathbf{m}_b$, $\mathbf{c}_b$ and $\mathbf{k}_b$ are the mass, damping and stiffness matrices of the base-isolation system, respectively. Also, vectors $\mathbf{u}_t$ and $\mathbf{u}_f$ are measured relative to the base, and $\mathbf{u}_b$ is the vector of base displacement relative to the ground motion. Matrices $\mathbf{M}$, $\mathbf{C}$ and $\mathbf{K}$ are presented in Eqs. (20a,b,c) and (20d).

3. Illustrative numerical analyses

3.1. Fluid–structure system verification

A computer program has been developed to compute the natural frequencies of liquid sloshing and coupled fluid–structure system. Several liquid storage tanks with various properties are examined to demonstrate the validity of the proposed modeling process. Numerical results are presented to express the variations of dynamic characteristics with different geometric dimensions of the system. These geometric dimensions consist of the height, radius, and thickness of the shell structure, and liquid depth. The analysis results of both broad and slender tanks are presented here.

The dimensions of the slender tank are: radius $R = 7.32$ m, height $h = 21.96$ m, and wall thickness $t = 0.0109$ m, with the mass density of the liquid $\rho = 1000\,\text{kg/m}^3$. The tank is made of steel whose properties are: Young's modulus $E = 206.7$ GPa, density $\rho_S = 7840\,\text{kg/m}^3$, and Poisson's ratio $= 0.3$.

The dimensions of the broad tank are: $R = 18.30$ m, $h = 12.20$ m, and $t = 0.0254$ m. The material properties of the broad tank are the same as those of the slender tank.

The comparison between the present study results and analytical results (Veletsos and Tang, 1987) is presented in Table 1, which shows good agreement between the two results.

To perform the verification in the time domain, seismic response analyses for both of the foregoing tanks were carried out using the horizontal acceleration component of the 1994 Newhall earthquake with a PGA of $0.678g$ (see Fig. 3). The summary of the maximum seismic responses of the foregoing tanks for the present study and the same model of Veletsos and Tang (1984) is presented in Table 2. Fig. 4 shows the plots of time histories of base shear for the slender tank considering the shell structure to be rigid and/or flexible, while Fig. 5 shows base shear variations for the broad tank. The results of the present study are in reasonable agreement with the results of Veletsos and Tang (1984, 1987). As a result, Figs. 4 and 5 show that the effect of tank shell flexibility on the convective component of the response is negligible. Accordingly, in computing the response of a flexible liquid tank, the convective component can be computed assuming the tank wall to be rigid and only the effect of tank shell flexibility on the impulsive component should be considered.

Table 1
Natural frequencies ω (Hz) of slender and broad tanks considering liquid sloshing for $\cos\theta$ dominant circumferential mode

3-D mode number	Slender tank				Broad tank			
	Liquid sloshing	Present study	Veletsos and Tang (1987)	Error (%)	Liquid sloshing	Present study	Veletsos and Tang (1987)	Error (%)
1	0.250	3.60	3.56	1.12	0.145	6.22	6.18	0.64
2	0.425	10.51	10.45	0.57	0.269	11.35	11.28	0.62
3	0.538	15.65	15.55	0.64	0.340	15.23	15.10	0.86

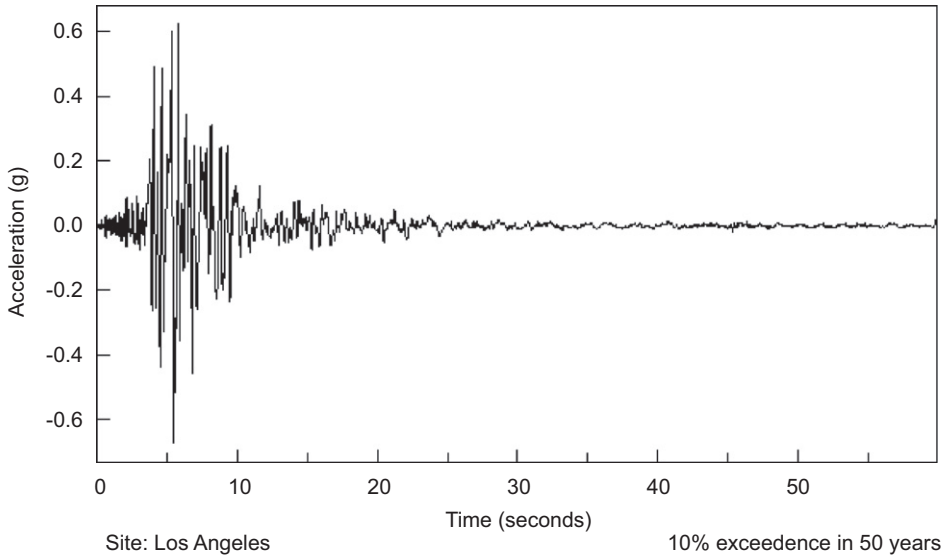

Fig. 3. Ground acceleration time history (1994 Newhall earthquake).

Table 2
Seismic response of slender and broad flexible tanks in the time domain

Parameters	Slender tank			Broad tank		
	Time (s)	Present study	Veletsos and Tang (1984)	Time (s)	Present study	Veletsos and Tang (1984)
$Q_{max}(N)$	5.96	14.15×10^6	14.28×10^6	5.809	50.22×10^6	49.98×10^6
$M_{max}(N_m)$	5.96	17.66×10^7	17.45×10^7	5.809	31.83×10^7	31.12×10^7
η_{max}	8.47	181.35	184.65	20.95	232.85	232.85

Q_{max}: maximum base shear; M_{max}: maximum overturning moment; η_{max}: maximum sloshing height.

3.2. Usage of base-isolated liquid storage tanks on a rigid foundation

In this section, seismic analyses are carried out to observe the effects of base-isolation system on the seismic response of liquid storage tanks with different geometric dimensions. We consider the first tank of the previous section with the same material properties. The influence of aspect ratio (height to radius) on the dynamic characteristics of base-isolated liquid storage tanks is studied employing tanks of the same radius $R = 7.32$ m and different heights with a full depth of water (10% left for the sloshing wave). The aspect ratios are 3 (slender tank), 1.5 (medium tank) and 0.75 (broad tank); i.e., the heights are 21.96, 10.98, 5.49 m, respectively. The material properties of the whole system are shown in Table 3.

The following analyses consist of frequency domain analyses and time domain seismic response analyses of the fluid–structure behavior of foregoing cylindrical tanks.

3.2.1. Analyses in the frequency domain

The analyses in the frequency domain for different aspect ratios are performed to observe the effect of geometric dimensions on the behavior of the whole system. Fig. 6 shows the relative displacements between the foundation and the bottom of the tank for various aspect ratios assuming the tank wall to be rigid and/or flexible. In this analysis, linear base-isolators are considered whose horizontal stiffness is 4.0×10^7 kg/m (Case I). As may be observed from Fig. 6, the maximum relative displacement amplitudes occur in lower frequencies. Furthermore, these maximum amplitudes decrease as the frequencies increase. As a result, the main purpose of base-isolation designing is to absorb the most earthquake energy in the range of low frequencies. The magnification ratios in Fig. 6 from 0.0 to 1.0 Hz show the

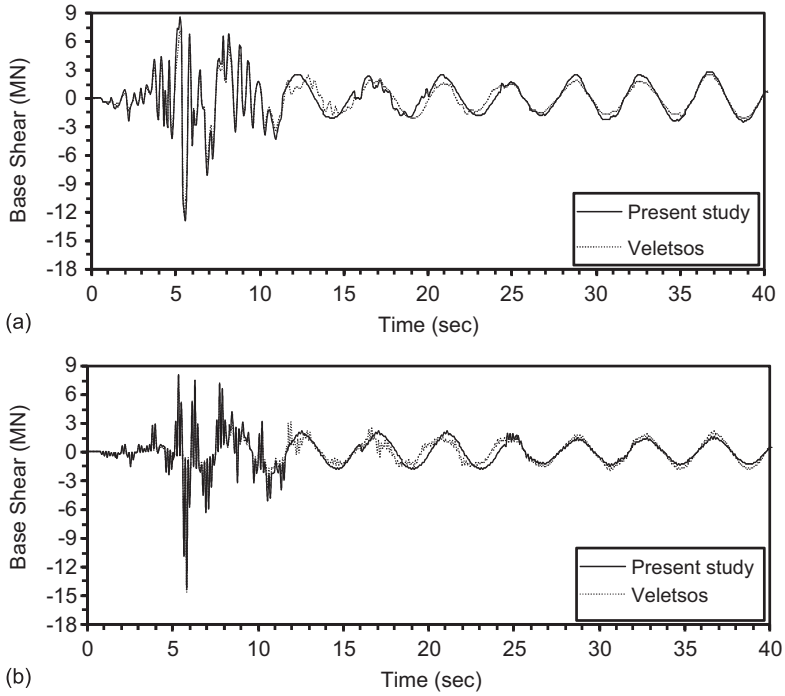

Fig. 4. Base shear time histories for the slender tank subjected to the 1994 Newhall earthquake: (a) rigid tank; (b) flexible tank.

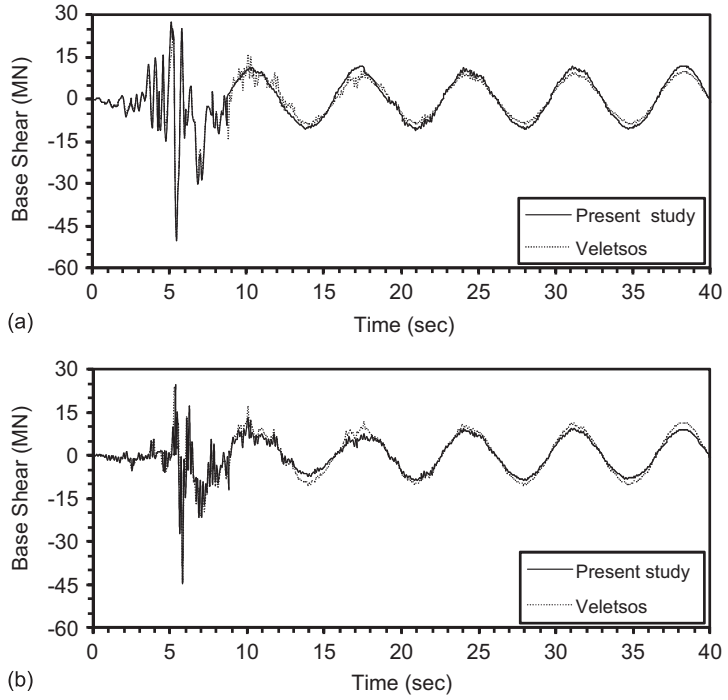

Fig. 5. Base shear time histories for the broad tank subjected to the 1994 Newhall earthquake: (a) rigid tank; (b) flexible tank.

natural frequencies of base-isolation of both rigid and flexible tanks for various aspect ratios. As the height of liquid tank increases, the effect of wall flexibility on the response of the base-isolation system is more considerable, and the amplitudes of relative response have less increase in comparison with those of rigid tanks. The natural frequencies of the

Table 3
Material properties of the whole system

Tank	Density	ρ_S (kg/m^3)	7840
	Poisson's ratio	v	0.3
	Young's modulus	E (GPa)	206.7
Base-isolation	Horizontal stiffness	K_{elastic} (kg/m)	4.0×10^7 (case I), 1.0×10^7 (case II)
	Vertical stiffness	K_v (kg/m)	1.0×10^{10}
	Horizontal damping	β_h	0.06
	Vertical damping	β_v	0.04
	Stiffness ratio	α	0.15
	Yield force	F_y (kg)	3.2×10^5 (case I), 0.8×10^5 (case II)
Liquid	Density	ρ (kg/m^3)	1000

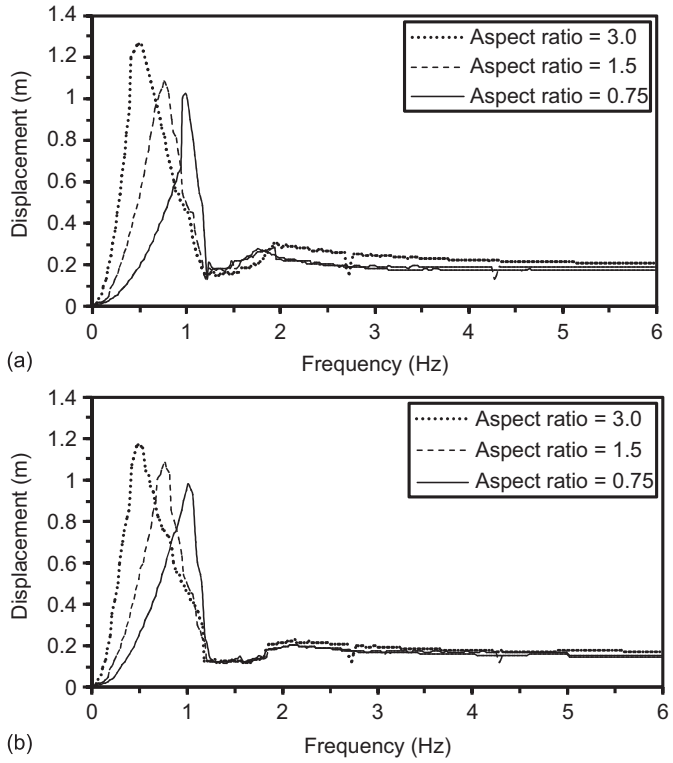

Fig. 6. Relative displacements between the foundation and the bottom of the tank for different aspect ratios (considering case I isolation system): (a) rigid tank; (b) flexible tank.

0.75, 1.5 and 3 liquid-filled tank aspect ratios are 0.99, 0.74 and 0.56 Hz, respectively. They are not much different from those of single-degree-of-freedom systems, which are 0.98, 0.72 and 0.55 Hz, based on Eq. (23). This is because the base-isolators govern the behavior of the whole system, with

$$f = \frac{1}{2\pi}\sqrt{\frac{k}{m}} \tag{23}$$

in which k and m are the isolation system stiffness and total liquid and tank masses, respectively.

To compare the responses of the system according to variations in the stiffness of the base-isolators, we divide the stiffness of the base-isolators by 4 (case II) and re-analyze the liquid storage tanks. The relative displacements between the foundation and the bottom of both rigid and flexible tanks for new stiffness are shown in Fig. 7. As the stiffness of

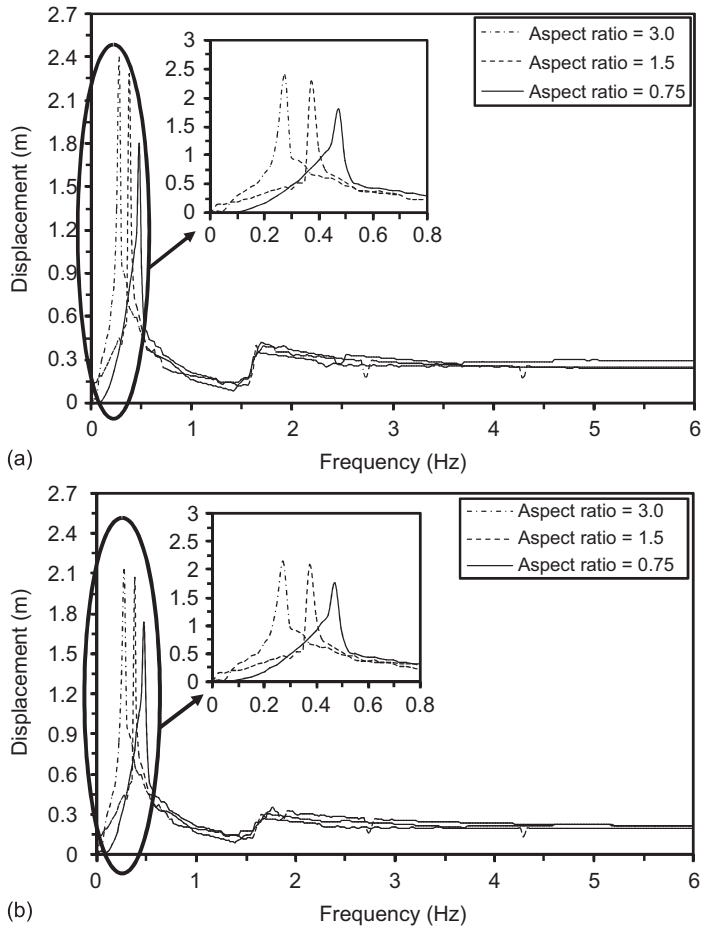

Fig. 7. Relative displacements between the foundation and the bottom of the tank for different aspect ratios (considering case II isolation system): (a) rigid tank; (b) flexible tank.

the base-isolation system decreases, the natural frequencies decrease and the amplitudes of relative displacements increase.

Analyses in the frequency domain show that base-isolation system is more effective when the stiffness of base-isolators is small. However, the stiffness of isolators should assure the stability of liquid storage tank.

3.2.2. *Analyses in the time domain*

A time-history analysis for different aspect ratios is carried out using the 1994 Newhall earthquake as input ground motion. In order to obtain the dynamic response of the structure in the time domain, the inverse Fourier transformation is used. The effects of liquid tank aspect ratios and base-isolators are studied in this section. Verifications on the application of frequency domain analysis for the non-linear behavior of base-isolated liquid storage tanks are given in Section 3.2.2.6.

3.2.2.1. Base isolator seismic response. Fig. 8 shows the relative displacements between the structure bottom and the ground for various aspect ratios assuming the isolated tanks of case I. The peak isolator displacements are 0.0647, 0.0409 and 0.035 m, for the aspect ratios of 3, 1.5 and 0.75, respectively. This may indicate that the isolator displacement increases as the aspect ratio increases, particularly in the slender tank in comparison with the broad one.

The influence of stiffness variation of isolation system on the seismic response of liquid tanks is presented in Fig. 9. It is observed that for the isolated tanks of case I, when the aspect ratios are 3, 1.5 and 0.75, the maximum isolator displacements are 0.0647, 0.0409 and 0.035 m, respectively, while, for the isolated tanks of case II, for the foregoing aspect ratios, the corresponding displacements are 0.0818, 0.0488 and 0.0382, respectively. This may indicate that the

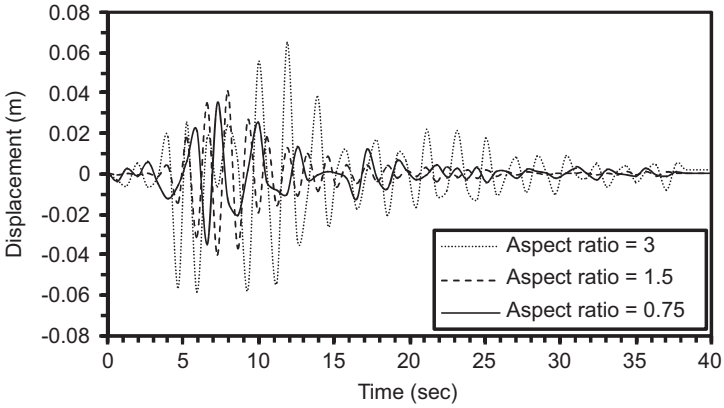

Fig. 8. Variation of isolator displacement for various aspect ratios of case I (subjected to the 1994 Newhall earthquake).

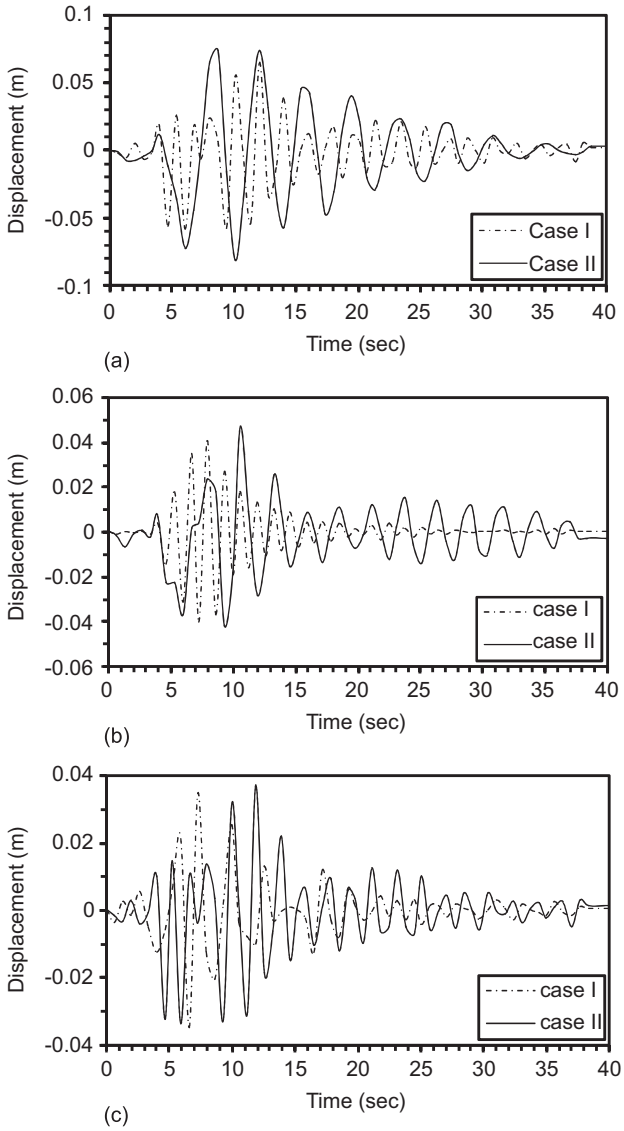

Fig. 9. Variation of isolator displacement of both cases I and II (subjected to the 1994 Newhall earthquake): (a) for the tank of aspect ratio 3; (b) for the tank of aspect ratio 1.5; (c) for the tank of aspect ratio 0.75.

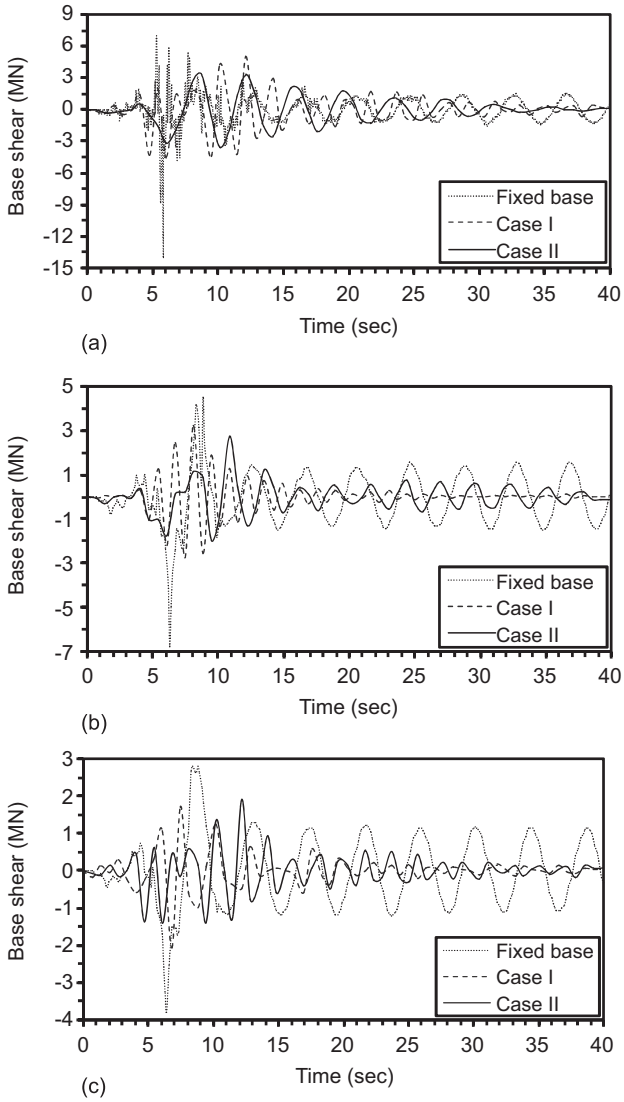

Fig. 10. Base shear time history considering various base isolator conditions (subjected to the 1994 Newhall earthquake): (a) for the tank of aspect ratio 3; (b) for the tank of aspect ratio 1.5; (c) for the tank of aspect ratio 0.75.

rate of increase of isolator displacement of more flexible isolators is more than those of stiffer isolators, as the aspect ratio increases.

3.2.2.2. Seismic base shears. Fig. 10 shows the time variation of base shears for the various base-isolation conditions. The peak base shears, assuming non-isolated model, are 14.01, 6.85 and 3.81 MN when the aspect ratios are 3, 1.5 and 0.75, respectively. For the isolated tanks of case I for the foregoing aspect ratios, the corresponding base shears are 4.95, 3.21 and 2.07 MN, respectively. On the other hand, the analogous base shears, assuming isolated tanks of case II, are 3.59, 2.70 and 1.89 MN, respectively. As a conclusion, for the isolated tanks of case I, the peak base shears reduce by 64.66%, 53.13% and 45.52% when the aspect ratios are 3, 1.5 and 0.75, respectively. Similarly, for the isolated tanks of case II, the corresponding reduction is by 74.37%, 60.58% and 50.26%, respectively. The above results indicate that due to base-isolation base shear is reduced considerably. Furthermore, the reduction in base shear is comparatively more in slender tanks. It is also obvious that variation in base isolator stiffness has more effect on the seismic response of slender tanks.

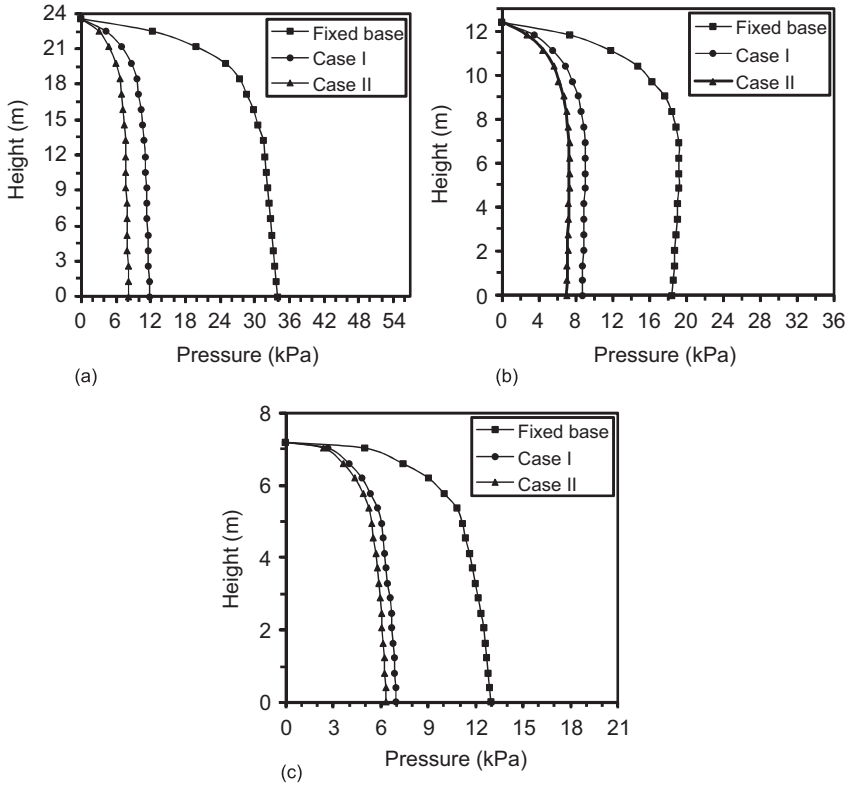

Fig. 11. Distributions of hydrodynamic pressure for rigid wall tanks: (a) for the tank of aspect ratio 3; (b) for the tank of aspect ratio 1.5; (c) for the tank of aspect ratio 0.75.

3.2.2.3. Seismic hydrodynamic pressure distribution. When the maximum base shears occur, the distribution of hydrodynamic pressure due to ground motion is shown in Fig. 11, assuming the tank wall to be rigid. The foregoing distributions for flexible tank structures are shown in Fig. 12.

The maximum hydrodynamic pressures for rigid wall tanks, assuming non-isolated model, are 34.03, 19.25 and 13.01 kPa when the aspect ratios are 3, 1.5 and 0.75, respectively. For the isolated tanks of case I, for the foregoing aspect ratios, the corresponding hydrodynamic pressures are 11.90, 9.04 and 7.02 kPa, respectively. The analogous hydrodynamic pressures, assuming isolated tanks case II, are 8.16, 7.31 and 6.37 kPa, respectively.

Similarly, considering the flexibility of the tank walls, the prior maxima for the non-isolated models are 36.25, 19.11 and 12.35 kPa, respectively. The corresponding maxima for the isolated tanks of case I are 14.34, 9.55 and 6.91 kPa, while for the isolated tanks of case II the analogous maxima are 11.61, 8.40 and 6.41 kPa, respectively. In order to investigate the reduction quantities of maximum hydrodynamic pressures in both rigid and flexible tanks for different isolation conditions, Fig. 13 has been drawn. Results indicate that due to base-isolation the maximum hydrodynamic pressure is reduced considerably. Moreover, the reduction percentage in the maximum hydrodynamic pressure is comparatively more significant in slender tanks. The comparative results indicate that the above-mentioned reduction is slightly more for rigid tanks in comparison with flexible tanks, especially as the stiffness of the base-isolation system decreases.

3.2.2.4. Liquid surface displacement. To estimate the contribution of sloshing effects on the hydrodynamic pressure, one may simply eliminate its effects from analysis by replacement of sloshing boundary condition Eqs. (2) and (5) with the equation $\eta(x,y,t) = 0$ in the BEM analysis. This simple modification results in the case in which no sloshing displacement is taken into account. Differences between the results of this case with the results obtained by considering sloshing boundary conditions reveal the distributions of hydrodynamic pressure considering sloshing effects only.

Fig. 14 shows the hydrodynamic pressure, due to the maximum sloshing displacement, acting on the tank wall. The maximum sloshing pressures, assuming non-isolated (fixed-base) model, are 18.10, 15.86 and 16.73 kPa, when the aspect ratios are 3, 1.5 and 0.75, respectively. For the isolated tanks of case I, for the foregoing aspect ratios, the corresponding

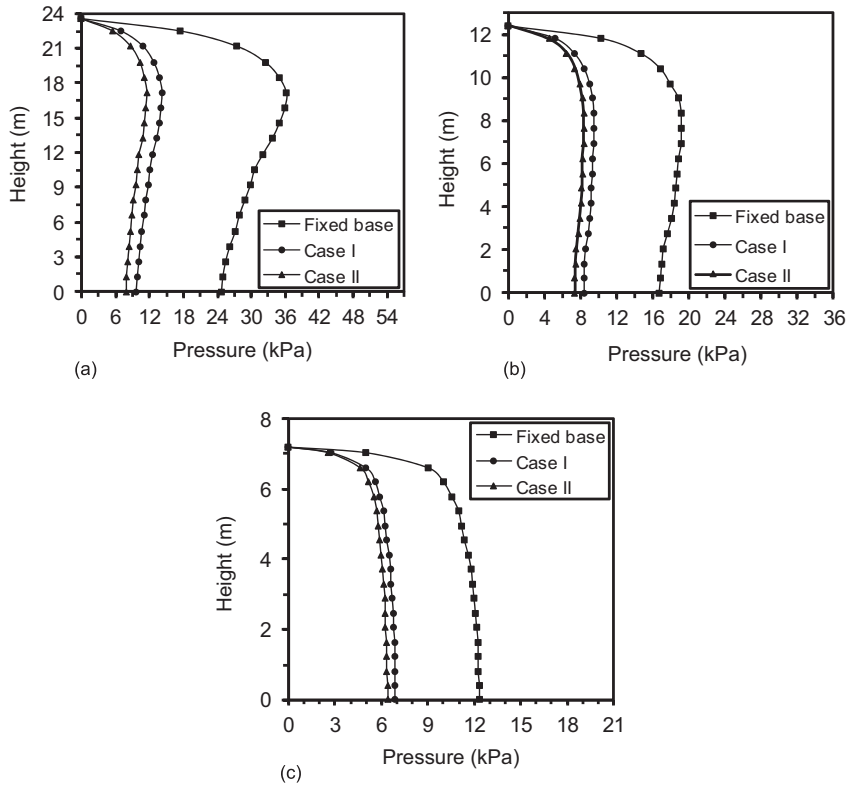

Fig. 12. Distributions of hydrodynamic pressure for flexible wall tanks: (a) for the tank of aspect ratio 3; (b) for the tank of aspect ratio 1.5; (c) for the tank of aspect ratio 0.75.

hydrodynamic pressures are 19.05, 16.33 and 17.07 kPa, respectively. The analogous hydrodynamic pressures, assuming isolated tanks of case II, are 20.50, 16.97 and 17.57 kPa, respectively. This shows that for the isolated tanks of case I the maximum sloshing pressures increase by 5.24%, 2.96% and 2.03%, when the aspect ratios are 3, 1.5 and 0.75, respectively. Similarly, for the isolated tanks of case II, the corresponding reductions are 13.20%, 6.99% and 5.02%, respectively. The comparative results between cases I and II show that the maximum liquid surface displacement considerably increases in slender tanks. Also, the liquid surface displacement is more affected by isolation effects in slender tanks.

3.2.2.5. Whole system natural frequencies. In order to observe the behavior of the whole system, assume a harmonic acceleration time history $\ddot{u}_g(t) = \sin(\omega t)$ as input ground motion. Fig. 15 shows the relative displacements between the foundation and the bottom of the tank for different aspect ratios (considering case I isolation system). The natural frequencies of the 0.75, 1.5 and 3 liquid-filled tank aspect ratios are 0.96, 0.74 and 0.53 Hz, for the primary range of stiffness, respectively. Using Eq. (23), the corresponding frequencies of single-degree-of-freedom systems are 0.98, 0.72 and 0.55 Hz, respectively. Also, for the secondary range of stiffness, the foregoing natural frequencies are 0.34, 0.25 and 0.20 Hz, respectively, while the corresponding frequencies of single-degree-of-freedom systems are 0.37, 0.27 and 0.21 Hz. These comparative results indicate that the behavior of the whole system is close to the single-degree-of-freedom system considering biaxial stiffness behavior of the isolation system.

3.2.2.6. Verification of the proposed method. It is a common way to solve the whole system dynamic response (hydrodynamic interaction problem coupled with base-isolation) in the time domain. In this research, frequency domain formulations of BE–FE methods are employed to make more accurate sense of the hydrodynamic pressure component due to sloshing effect, which depends very strongly on the frequency spectrum of the ground motion. For this purpose, frequency domain analysis (i.e., forward and inverse Fourier Transformation) is performed for short consecutive time steps (e.g., 0.1 s) of ground motion time history. This process permits the algorithm to follow the correct path of a non-linear phenomenon. Fig. 16 shows the comparison between the results of this research and the time domain analysis of

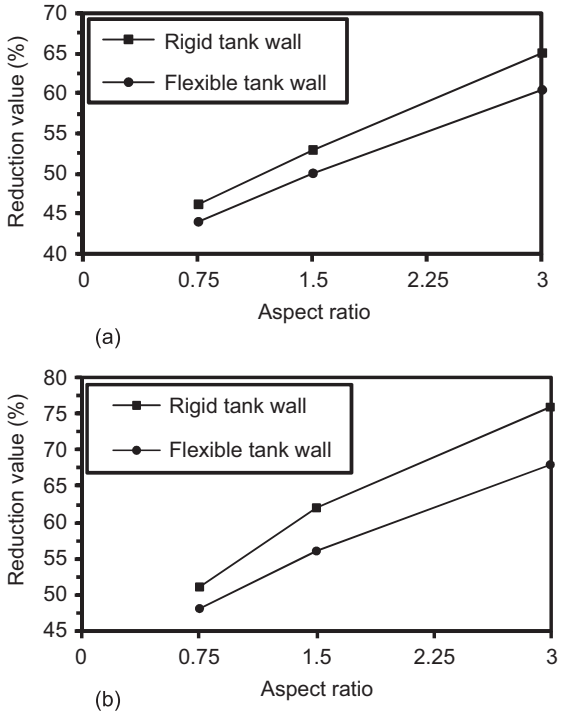

Fig. 13. Reduction values in the maximum hydrodynamic pressures for different conditions: (a) base isolation case I; (b) base isolation case II.

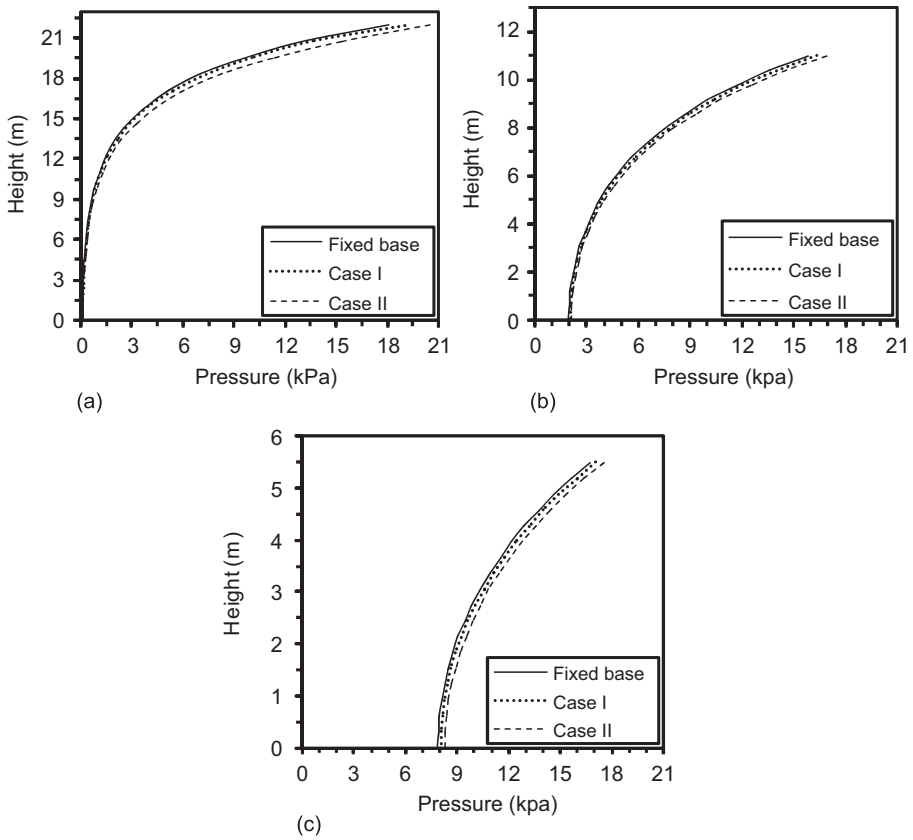

Fig. 14. Distributions of hydrodynamic pressure considering sloshing effects only: (a) for the tank of aspect ratio 3; (b) for the tank of aspect ratio 1.5; (c) for the tank of aspect ratio 0.75.

an isolated liquid tank done by Cho et al. (2004), while Fig. 17 plots the liquid sloshing heights under the same conditions. Good agreement between the two results indicates the validity of the present algorithm.

The hysteretic behavior of the base-isolation system as a relationship between isolation displacement and isolation shear force is plotted in Fig. 18. The comparative results between cases I and II indicate that earthquake energy dissipation depends on the base-isolation properties, especially in slender tanks.

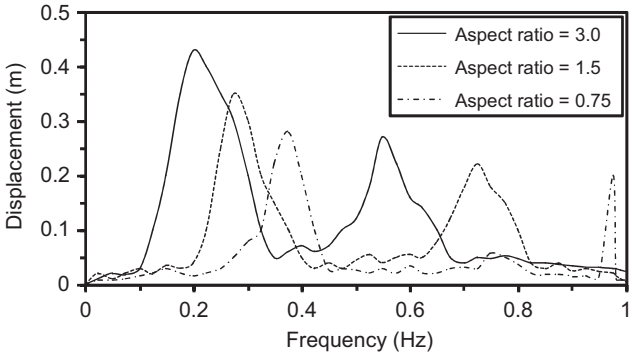

Fig. 15. Variation of isolator displacement for nonlinear properties of case I isolation system.

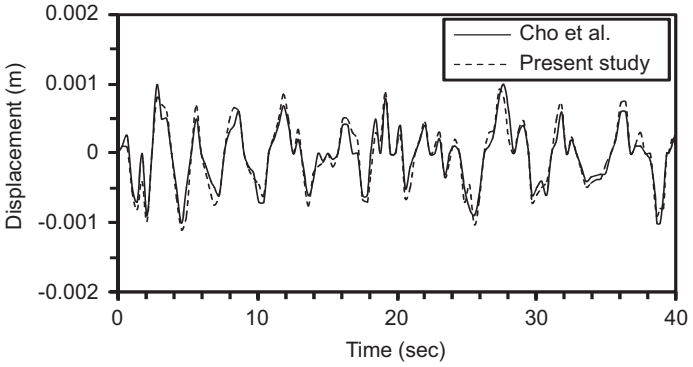

Fig. 16. Seismic base isolated tank radial displacement.

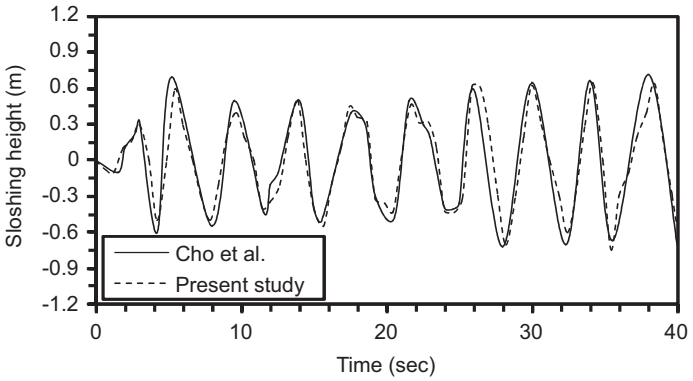

Fig. 17. Sloshing liquid heights.

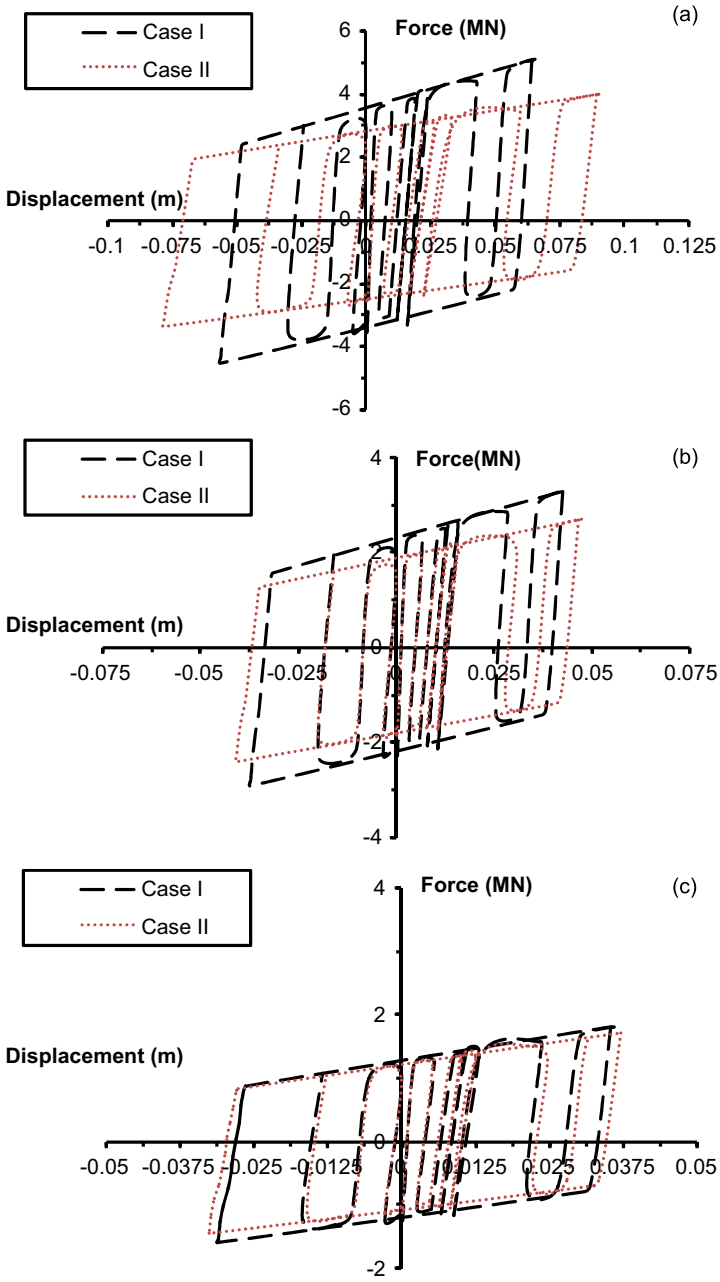

Fig. 18. Force–displacement relation diagrams for the isolation system: (a) slender tank; (b) medium tank; (c) broad tank.

4. Conclusions

A three-dimensional numerical procedure has been developed to analyze the dynamic response of base-isolated liquid storage tanks on rigid foundation, under the excitation of horizontal seismic waves. This is achieved by transforming the boundary element equations governing the liquid region into an equivalent liquid mass matrix, which is then combined with the shell finite-element equations of motion. The governing set of equations of motion is then solved for the fluid–structure interaction problem. The proposed numerical method predicts the seismic response of the isolated cylindrical liquid storage tanks with considerably less computational effort due to the reduction of problem dimensions

in the BEM. Various numerical examples are given to prove the accuracy and validity of the present method. The following conclusions are drawn by processing the results of the present study.

1. It is noticed that due to the base-isolation system the base shear is significantly reduced, especially in slender tanks.
2. When the liquid storage tank aspect ratio (considering constant radius) increases, the relative displacement between the bottom of the structure and the ground increases, while the natural frequency of the base-isolation system decreases.
3. In the frequency domain analyses, it is observed that the natural frequencies of the isolated tanks are not much different from those of single-degree-of-freedom system. This indicates that base-isolators govern the behavior of the whole system. Therefore, for design purposes it is appropriate to use the foregoing idea and estimate the natural frequency of the whole system. This is specifically the case for slender tanks, in which the effect of liquid surface displacement is of less importance in comparison with broad tanks.
4. It is proposed to use the base-isolation system with smaller stiffness in order to be in the low-frequency range of seismic energy, while considering the stability of the storage tank and allowable displacements of base isolator in the design of superstructure.
5. The reduction in maximum seismic response and the effectiveness of seismic isolation (i.e., increase in flexibility) is comparatively more significant as the aspect ratio increases.
6. The maximum liquid surface displacement increases with increase of isolator flexibility, and it is more important in slender tanks.

References

Amabili, M., Païdoussis, M.P., Lakis, A.A., 1998. Vibrations of partially filled cylindrical tanks with ring-stiffeners and flexible bottom. Journal of Sound and Vibration 213, 259–299.

Brebbia, C.A., Dominguez, J., 1992. Boundary Elements, An Introductory Course. CMP & McGraw-Hill, New York.

Chalhoub, M.S., Kelly, J.M., 1990. Shake table test of cylindrical water tanks in base-isolated structures. ASCE Journal of Engineering Mechanics 116, 1451–1472.

Cho, K.H., Kim, M.K., Lim, Y.M., Cho, S.Y., 2004. Seismic response of base-isolated liquid storage tanks considering fluid–structure–soil interaction in time domain. Soil Dynamics and Earthquake Engineering 24, 839–852.

Fischer, F.D., Rammerstorfer, F.G., 1999. A refined analysis of sloshing effects in seismically excited tanks. International Journal of Pressure Vessels and Piping 76, 693–709.

Haroun, M.A., Chen, W., 1996. Large amplitude liquid sloshing in seismically excited tanks. Earthquake Engineering and Structural Dynamics 25, 653–669.

Haroun, M.A., Ellaithy, H.M., 1985. Model for flexible tanks undergoing rocking. ASCE Journal of Engineering Mechanics 111, 143–157.

Haroun, M.A., Housner, G.W., 1981. Seismic design of fluid storage tanks. ASCE Proceedings of Journal of Technical Councils, 191–207.

Haroun, M.A., Housner, G.W., 1982. Dynamic characteristics of liquid storage tanks. ASCE Journal of Engineering Mechanics 108, 783–800.

Housner, G.W., 1963. The dynamic behavior of water tanks. Bulletin of the Seismological Society of America 53, 381–387.

Jadhav, M.B., Jangid, R.S., 2004. Response of base-isolated liquid storage tanks. Shock and Vibration 11, 33–45.

Jadhav, M.B., Jangid, R.S., 2006. Response of base-isolated liquid storage tanks to near-fault motions. Structural Engineering and Mechanics 23, 615–634.

Kelly, J.M., 1993. Earthquake-Resistant Design with Rubber. Springer, New York.

Kim, N.S., Lee, D.G., 1995. Pseudodynamic test for evaluation of seismic performance of base-isolated liquid storage tanks. Engineering Structures 17, 198–208.

Kim, M.K., Lim, Y.M., Cho, S.Y., Cho, K.H., Lee, K.W., 2002. Seismic analysis of base-isolated liquid storage tanks using the BE–FE–BE coupling technique. Soil Dynamics and Earthquake Engineering 22, 1151–1158.

Lay, K.S., 1993. Seismic coupled modeling of axisymmetric tanks containing liquid. ASCE Journal of Engineering Mechanics 119, 1747–1761.

Liang, B., Tang, J.-X., 1994. Vibration studies of base-isolated liquid storage tanks. Computers and Structures 52, 1051–1059.

Livaoğlu, R., Doganğün, A., 2006. Simplified seismic analysis procedures for elevated tanks considering fluid–structure–soil interaction. Journal of Fluids and Structures 22, 421–439.

Malhotra, P.K., 1997a. Method for seismic base-isolation of liquid-storage tanks. ASCE Journal of Structural Engineering 123, 113–116.

Malhotra, P.K., 1997b. New method for seismic isolation of liquid-storage tanks. Earthquake Engineering and Structural Dynamics 26, 839–847.

Malhotra, P.K., Veletsos, A.S., 1994. Uplifting analysis of base plates in cylindrical tanks. ASCE Journal of Structural Engineering 120, 3489–3505.

Malhotra, P.K., Wenk, T., Wieland, M., 2000. Simple procedure for seismic analysis of liquid storage tanks. Structural Engineering International 10, 197–201.

Papaspyrou, S., Karamanos, S.A., Valougeorgis, D., 2004. Response of half-full horizontal cylinders under transverse excitation. Journal of Fluids and Structures 19, 985–1003.

Shenton, H.W., Hampton, F.P., 1999. Seismic response of isolated elevated water tanks. ASCE Journal of Structural Engineering 125, 965–976.

Shivakumar, P., Veletsos, A.S., 1995. Dynamic response of rigid tanks with inhomogeneous liquid. Earthquake Engineering and Structural Dynamics 24, 991–1015.

Shrimali, M.K., Jangid, R.S., 2002. Seismic response of liquid storage tanks isolated by sliding bearings. Engineering Structures 24, 909–921.

Shrimali, M.K., Jangid, R.S., 2004. Seismic analysis base-isolated liquid storage tanks. Journal of Sound and Vibration 275, 59–75.

Tang, Y., 1994. Mechanical models for tanks containing two liquids. Argonne National Laboratory, Report No. ANL/RE/CP-80722, pp. 1–13.

Veletsos, A.S., Shivakumar, P., 1993. Sloshing response of layered liquids in rigid tanks. Earthquake Engineering and Structural Dynamics 22, 801–821.

Veletsos, A.S., Shivakumar, P., 1995. Hydrodynamic effects of rigid tanks containing layered liquids. Earthquake Engineering and Structural Dynamics 24, 835–860.

Veletsos, A.S., Tang, Y., 1984. Seismic response and design of liquid storage tanks: guidelines for the seismic design of oil and gas pipeline systems. ASCE Technical Council on Lifeline Earthquake Engineering, 443–461.

Veletsos, A.S., Tang, Y., 1987. Rocking response of liquid storage tanks. ASCE Journal of Engineering Mechanics 113, 1774–1792.

Zienkiewicz, O.C., Taylor, R.L., 2000. The Finite Element Method. Butterworth and Heinmann, Oxford.